

Excited states of diphenylacetylene (tolan)

Near and vacuum UV polarization spectroscopy

Nguyen, Duy Duc; Jones, Nikola C.; Hoffmann, Søren V.; Spanget-Larsen, Jens

Published in:
European Journal of Chemistry

DOI:
[10.5155/eurjchem.15.2.87-92.2546](https://doi.org/10.5155/eurjchem.15.2.87-92.2546)

Publication date:
2024

Document Version
Publisher's PDF, also known as Version of record

Citation for published version (APA):
Nguyen, D. D., Jones, N. C., Hoffmann, S. V., & Spanget-Larsen, J. (2024). Excited states of diphenylacetylene (tolan): Near and vacuum UV polarization spectroscopy. *European Journal of Chemistry*, 15(2), 87-92.
<https://doi.org/10.5155/eurjchem.15.2.87-92.2546>

General rights

Copyright and moral rights for the publications made accessible in the public portal are retained by the authors and/or other copyright owners and it is a condition of accessing publications that users recognise and abide by the legal requirements associated with these rights.

- Users may download and print one copy of any publication from the public portal for the purpose of private study or research.
- You may not further distribute the material or use it for any profit-making activity or commercial gain.
- You may freely distribute the URL identifying the publication in the public portal.

Take down policy

If you believe that this document breaches copyright please contact rucforsk@kb.dk providing details, and we will remove access to the work immediately and investigate your claim.


[View Journal Online](#)
[View Article Online](#)

Excited states of diphenylacetylene (tolan): Near and vacuum UV polarization spectroscopy

Duy Duc Nguyen ^{1,#}, Nykola C. Jones ², Søren Vrønning Hoffmann ²,
and Jens Spanget-Larsen ^{1,*}

¹ Department of Science and Environment, Roskilde University, Universitetsvej 1, DK-4000 Roskilde, Denmark

² Centre for Storage Ring Facilities (ISA), Department of Physics and Astronomy, Aarhus University, Ny Munkegade 120, DK-8000 Aarhus C, Denmark

* Corresponding author at: Department of Science and Environment, Roskilde University, Universitetsvej 1, DK-4000 Roskilde, Denmark.

Present affiliation: Duy Duc Nguyen, Intertek Vietnam Limited, Tan Binh District, Ho Chi Minh City, Vietnam.

e-mail: spanget@ruc.dk (J. Spanget-Larsen).

RESEARCH ARTICLE



doi 10.5155/eurjchem.15.2.87-92.2546

Received: 9 March 2024

Received in revised form: 28 March 2024

Accepted: 4 April 2024

Published online: 30 June 2024

Printed: 30 June 2024

KEYWORDS

MCD B-terms
Near and vacuum UV
Synchrotron radiation
Stretched polyethylene
Polarization spectroscopy
LCOAO and TD-DFT calculations

ABSTRACT

The UV absorbance spectrum of the important chromophore diphenylacetylene (tolan) is investigated by Synchrotron Radiation Linear Dichroism (SRLD) spectroscopy using stretched polyethylene as an anisotropic solvent. The investigation covers the range of 58,000–28,000 cm^{−1} (172–360 nm). The observed linear dichroism provides information on the transition moment directions of the four main absorbance bands A, B, C, and D at 33,300, 44,400, 51,000, and 57,000 cm^{−1} (300, 225, 196, and 175 nm). The experimental wavenumbers, intensities, and polarization directions are compared with the results of quantum chemical calculations using the semiempirical all-valence-electrons method Linear Combination of Orthogonalized Atomic Orbitals (LCOAO) and Time-Dependent Density Functional Theory (TD-DFT) with the functional CAM-B3LYP. Magnetic Circular Dichroism (MCD) B-terms predicted with LCOAO suggest that a number of optically weak transitions may be observed by MCD spectroscopy.

Cite this: *Eur. J. Chem.* **2024**, *15*(2), 87-92

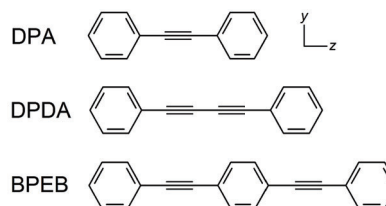
Journal website: www.eurjchem.com

1. Introduction

Diphenylacetylene (tolan, DPA, [Scheme 1](#)) is a prototype of the oligo phenylene-ethynylene (OPE) systems which are of great interest in the fields of molecular wires and other molecular-based electronic devices [1-4]. The photophysical, photochemical, and spectroscopic properties of DPA have been studied for decades; for entries in the literature, see references [5-14]. We have previously studied the excited electronic states of the related compounds diphenyldiacetylene (DPDA) [15] and 1,4-bis(phenylethynyl)benzene (BPB) [16] ([Scheme 1](#)). In the present publication, we report the results of a similar study of DPA, investigating the ground state absorbance spectrum by UV Synchrotron Radiation Linear Dichroism (SRLD) spectroscopy on molecular samples partially aligned in stretched polyethylene (PE). The measured LD provides information on the polarization directions of the observed transitions [17-22], and with synchrotron radiation [23,24] the investigated spectral range can be extended to about 58,000 cm^{−1} (172 nm).

The observed energies, intensities, and polarizations are compared with the results of theoretical calculations using the Linear Combination of Orthogonalized Atomic Orbitals

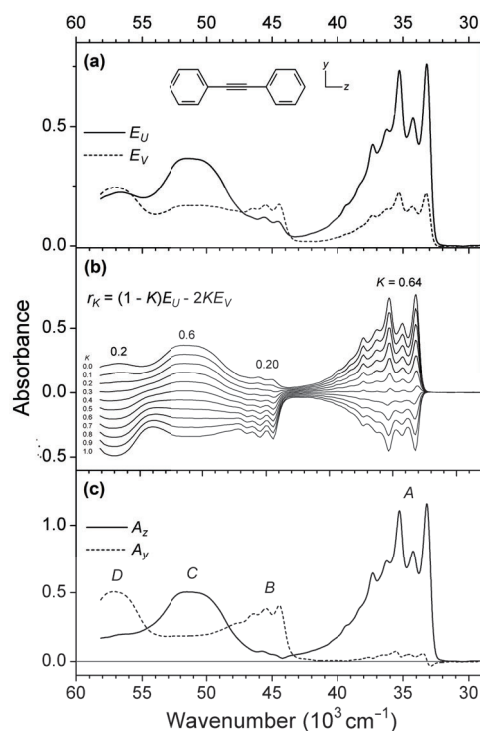
(LCOAO) model [25,26] and Time-Dependent Density Functional Theory (TD-DFT) [27-29] with the functional CAM-B3LYP [30]. The semiempirical all-valence-electrons LCOAO procedure was specifically developed for the prediction of the electronic absorption and Magnetic Circular Dichroism (MCD) spectra [31] of conjugated hydrocarbons [25,26] and has been applied to several π -systems with triple-bonded linkages [16, 26,32,33]. Additional data provided as Electronic supplementary information (ESI) is referred to in the ensuing text as [Sup. S1-S5](#).



Scheme 1. Diphenylacetylene (tolan, DPA), diphenyldiacetylene (DPDA), and 1,4-bis(phenylethynyl)benzene (BPB).

Table 1. Observed features of the SRLD spectrum of diphenylacetylene (DPA) and vertical electronic transitions predicted with LCOAO. A graphical representation of the predicted transitions is shown in Figure 2 (see also Sup. S4).

Observed				LCOAO ^a				
	$\tilde{\nu}$ ^b	Abs ^c	Pol ^d	Term	$\tilde{\nu}$ ^b	f ^e	B ^f	Leading configurations ^g
A	33.2 ^h	1.18 ^h	z	1 ¹ B _{1u}	34.1	1.60	-0.63	98%[3b _{3u} →3b _{2g}]
				1 ¹ B _{2u}	36.7	1·10 ⁻³	+1.07	40%[1a _u →3b _{2g}], 35%[3b _{3u} →2b _{1g}]
				1 ¹ B _{3g}	36.8	0	0	40%[1b _{1g} →3b _{2g}], 35%[3b _{3u} →2a _u]
				2 ¹ A _g	46.5	0	0	64%[3b _{3u} →4b _{3u}], 17%[2b _{2g} →3b _{2g}]
				3 ¹ A _g	46.9	0	0	69%[2b _{2g} →3b _{2g}], 24%[3b _{3u} →4b _{3u}]
B	44.4 ^h	0.42 ^h	y	2 ¹ B _{3g}	48.1	0	0	49%[1b _{1g} →3b _{2g}], 49%[3b _{3u} →2a _u]
				2 ¹ B _{2u}	48.7	0.87	-0.65	49%[1a _u →3b _{2g}], 49%[3b _{3u} →2b _{1g}]
C	51	0.50	z	2 ¹ B _{1u}	52.2	0.81	+2.11	43%[1a _u →2b _{1g}], 42%[1b _{1g} →2a _u]
				4 ¹ A _g	56.0	0	0	40%[1b _{1g} →2b _{1g}], 40%[1a _u →2a _u]
				3 ¹ B _{2u}	56.1	0.04	-2.00	42%[1b _{1g} →4b _{3u}], 22%[2b _{2g} →2a _u]
				3 ¹ B _{3g}	56.1	0	0	43%[1a _u →4b _{3u}], 20%[2b _{2g} →2b _{1g}]
				3 ¹ B _{1u}	58.8	0.02	+0.58	53%[2b _{3u} →3b _{2g}], 42%[3b _{3u} →4b _{2g}]
				4 ¹ B _{3g}	60.3	0	0	58%[2b _{2g} →2b _{1g}], 34%[1a _u →4b _{3u}]
				4 ¹ B _{2u}	60.8	1.17	+8.72	57%[2b _{2g} →2a _u], 36%[1b _{1g} →4b _{3u}]
D	57.1	0.51	y	4 ¹ B _{1u}	61.6	0.48	-8.58	79%[2b _{2g} →4b _{3u}], 6%[3b _{3u} →4b _{2g}]
				5 ¹ A _g	63.6	0	0	50%[1b _{1g} →2b _{1g}], 50%[1a _u →2a _u]

^a 16 lowest transitions, complete list provided as Sup. S4.^b Peak wavenumber in 1000 cm⁻¹.^c Peak absorbance estimated from the partial absorbance curves in Figure 1c.^d Polarization direction.^e Oscillator strength.^f MCD B-term in 10⁻³ β_e D²/cm⁻¹ (β_e = Bohr magneton, D = Debye).^g π-π* configurations, orbital energies and diagrams in Figure 3.^h Onset.**Figure 1.** (a) Absorbance curves measured with polarized light for diphenylacetylene (DPA) in stretched polyethylene. E_U and E_V indicate the absorbance measured with the stretching direction U parallel and perpendicular to the electric vector of the radiation. (b) Family of reduced absorbance curves r_K according to Equation 1 with K varying from 0 to 1 in steps of 0.1. (c) Partial absorbance curves A_y and A_z as defined in Equations 2 and 3, indicating y - and z -polarized absorbance.

2. Experimental

DPA [CAS 501-65-5] (98%) was purchased from Sigma-Aldrich. The spectroscopic purity of the substance was checked by comparison with the reference spectra available online [34]. Low-density polyethylene (PE) was obtained from Hinnum Plast, Denmark, as a pure 100 μ m sheet material. DPA was introduced into the PE sample by submersion of a piece of the polymer sheet into a saturated solution of the compound in chloroform (Merck Uvasol) at room temperature for several

days. Subsequently, the chloroform was allowed to evaporate, and the crystalline deposits on the surface were removed with methanol (Merck Uvasol). The PE sample was finally uniaxially stretched by ca. 500%. A sample without solute was prepared in the same manner for use as a reference. More details on stretched PE samples can be found in the literature [17-22].

The Synchrotron Radiation Linear Dichroism (SRLD) spectrum of DPA was measured at room temperature in the range 58,000-28,000 cm⁻¹ (172-360 nm) on the CD1 beamline [23,24] at the storage ring ASTRID at the Centre for Storage Ring Facilities (ISA). Two absorbance curves were recorded as previously described [16] with the electric vector of the sample beam parallel (U) and perpendicular (V) to the stretching direction of the PE sample. The baseline-corrected absorbance curves $E_U(\tilde{\nu})$ and $E_V(\tilde{\nu})$ are shown in Figure 1a. The LD is defined as the difference between the two curves, $LD = E_U(\tilde{\nu}) - E_V(\tilde{\nu})$. A version of the spectrum with an indication of all peak wavenumbers and absorbance is provided in Sup. S1.

2.1. Theory/Calculation

The electronic transitions of DPA were computed with the semiempirical all-valence-electrons method LCOAO [25,26] and with TD-DFT [27-29] using the functional CAM-B3LYP [30]. LCOAO calculation was performed with the computer program published in Reference [35]; a complete LCOAO bibliography is given in Sup. S5. CAM-B3LYP calculations were carried out with the Gaussian 16 software package [36].

The LCOAO calculation included the interaction between all singly excited singlet configurations generated by the promotion of an electron from the occupied π to unoccupied π^* molecular orbitals (MOs), comprising 49 π - π^* configurations. In addition to transition energies, intensities, and polarization directions, this calculation provided predictions of MCD B-terms [26,31] for the computed electronic transitions. The input geometry for the LCOAO calculation was taken as the one optimized with CAM-B3LYP and the basis set AUG-cc-pVTZ (see below). The main transitions obtained with LCOAO are listed in Table 1 and visualized in Figure 2, a complete listing of all LCOAO results is provided as Sup. S4.

CAM-B3LYP and TD-CAM-B3LYP calculations were carried out with the basis sets AUG-cc-pVTZ and cc-pVTZ (with and without the inclusion of diffuse functions) [37,38]. The isotropic

Table 2. Vertical electronic transitions for diphenylacetylene (DPA) predicted with TD-CAM-B3LYP/AUG-cc-pVTZ. A graphical representation is provided as Sup. S2.

TD-CAM-B3LYP/AUG-cc-pVTZ ^a			
Term	$\tilde{\nu}^b$	f^c	Leading configurations ^d
1 ¹ B _{1u}	35.4	1.12	94%[3b _{3u} (π)→3b _{2g} (π^*)]
1 ¹ B _{2u}	40.9	2·10 ⁻⁴	49%[3b _{3u} (π)→2b _{1g} (π^*)], 32%[1a _u (π)→3b _{2g} (π^*)]
1 ¹ B _{3g}	41.2	0	44%[3b _{3u} (π)→2a _u (π^*)], 35%[1b _{1g} (π)→3b _{2g} (π^*)]
1 ¹ A _u	42.5	0	94%[8b _{2u} ($\pi_{C\equiv C}$)→3b _{2g} (π^*)]
1 ¹ B _{3u}	45.3	2·10 ⁻³	76%[3b _{3u} (π)→14a _g (σ^*)], 11%[3b _{3u} (π)→15a _g (σ^*)]
2 ¹ A _g	47.3	0	59%[3b _{3u} (π)→4b _{3u} (π^*)], 18%[2b _{2g} (π)→3b _{2g} (π^*)]
2 ¹ B _{2u}	48.7	0.52	48%[1a _u (π)→3b _{2g} (π^*)], 43%[3b _{3u} (π)→2b _{1g} (π^*)]
2 ¹ B _{3u}	51.5	0.01	66%[3b _{3u} (π)→15a _g (σ^*)], 13%[3b _{3u} (π)→14a _g (σ^*)]
2 ¹ B _{1u}	52.1	0.73	46%[1a _u (π)→2b _{1g} (π^*)], 41%[1b _{1g} (π)→2a _u (π^*)]
3 ¹ B _{3u}	55.4	5·10 ⁻³	54%[3b _{3u} (π)→17a _g (σ^*)], 33%[3b _{3u} (π)→16a _g (σ^*)]
3 ¹ B _{1u}	57.4	0.21	68%[3b _{3u} (π)→4b _{2g} (π^*)], 14%[2b _{3u} (π)→3b _{2g} (π^*)]
4 ¹ B _{3u}	57.7	8·10 ⁻³	93%[8b _{2u} ($\pi_{C\equiv C}$)→2b _{1g} (π^*)]
3 ¹ B _{2u}	58.2	0.02	56%[8b _{2u} ($\pi_{C\equiv C}$)→14a _g (σ^*)], 20%[8b _{2u} ($\pi_{C\equiv C}$)→15a _g (σ^*)]
4 ¹ B _{1u}	58.3	0.65	30% 2b _{3u} (π)→3b _{2g} (π^*)], 18%[3b _{3u} (π)→4b _{2g} (π^*)]
5 ¹ B _{3u}	58.4	0.03	32%[1b _{1g} (π)→9b _{2u} (σ^*)], 17%[3b _{3u} (π)→16a _g (σ^*)]
6 ¹ B _{3u}	58.7	0.05	24%[1b _{1g} (π)→9b _{2u} (σ^*)], 19%[3b _{3u} (π)→17a _g (σ^*)]
4 ¹ B _{2u}	59.5	0.10	37%[2b _{2g} (π)→2a _u (π^*)], 20%[1b _{1g} (π)→4b _{3u} (π^*)]
5 ¹ B _{2u}	61.0	0.50	43%[1b _{1g} (π)→4b _{3u} (π^*)], 21%[2b _{2g} (π)→2a _u (π^*)]
6 ¹ B _{2u}	61.7	0.02	84%[3b _{3u} (π)→3b _{1g} (π^*)]

^a Main transition only, complete list provided as Sup. S2.

^b Wavenumber in 1000 cm⁻¹.

^c Oscillator strength.

^d $\pi_{C\equiv C}$ indicates the in-plane π component of the triple-bond.

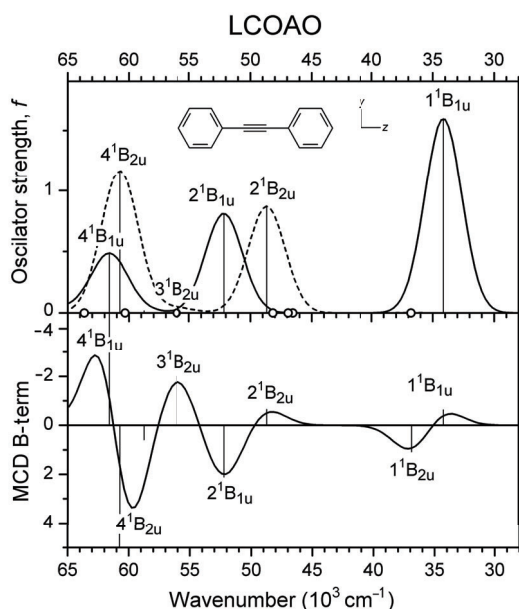


Figure 2. Gaussian convolutions of electronic transitions for diphenylacetylene (DPA) predicted with LCOAO.

influence of the solvent was approximated by the Polarizable Continuum Model IEFPCM [39-42] using *n*-hexadecane as the solvent [36]. The ground state equilibrium geometry of DPA was optimized under the assumption of D_{2h} symmetry with CAM-B3LYP using the respective basis sets and representing the dispersion effects by the model by Grimme [43] (keyword: empiricaldispersion=gd3bj [36]). The resulting nuclear coordinates are provided in Sup. S2 and Sup. S3 together with the results of frequency analyses. The TD-CAM-B3LYP calculations considered vertical transitions to the lowest 70 excited singlet states. The main transitions obtained with the basis set AUG-cc-pVTZ are listed in Table 2. Complete listings and graphical illustrations of all transitions computed with TD-CAM-B3LYP are provided as Sup. S2 and Sup. S3.

The convolutions of the predicted transitions are shown in Figure 2, Sup. S2, Sup. S3 and Sup. S4 were performed by assigning a Gaussian function to each excitation wavenumber with an area proportional to the oscillator strength or the MCD

B-term for that transition, using a constant standard deviation, $\sigma = 1,500 \text{ cm}^{-1}$.

3. Results and discussion

3.1. Linear dichroism: Orientation factors and polarization directions

The observed LD absorption curves $E_U(\tilde{\nu})$ and $E_V(\tilde{\nu})$ are shown in Figure 1a. Directional information that can be derived from the LD curves is given by the orientation factors $K_i = \langle \cos^2(\mathbf{M}_i, U) \rangle$, where (\mathbf{M}_i, U) is the angle of the dipole moment vector \mathbf{M}_i of transition i with the polymer stretching direction U and the pointed brackets indicate the average over all solute molecules in the light path [17-22]. The K_i values may be estimated by considering the ‘reduced’ absorbance curves $r_K(\tilde{\nu})$ (Equation 1) [19]:

$$r_K(\tilde{\nu}) = (1 - K)E_U(\tilde{\nu}) - 2KE_V(\tilde{\nu}) \quad (1)$$

The contribution from transition i vanishes from the linear combination $r_K(\tilde{\nu})$ for $K = K_i$, and the K_i value may thus be determined by visual inspection [19]. A family of curves $r_K(\tilde{\nu})$ for DPA with K ranging between the limits 0 and 1 is shown in Figure 1b, leading to determination of K_i values close to 0.64 and 0.20 for the main bands.

According to the D_{2h} molecular point group, dipole allowed transitions in DPA must be polarized along the molecular symmetry axes x , y , and z . We shall assume that the observed absorbance is primarily due to π - π^* transitions and thus polarized along the in-plane y and z axes (Scheme 1); this assumption is supported by the theoretical results (Tables 1 and 2, Sup. S2, Sup. S3, Sup. S4). Aromatic hydrocarbons tend to align in stretched PE according to their molecular dimensions [17-22] and we thus assign the observed K_i values 0.20 and 0.64 to the orientation factors of the short and long in-plane molecular axes y and z , $(K_y, K_z) = (0.20, 0.64)$. It is now possible to construct the partial absorbance curves $A_y(\tilde{\nu})$ and $A_z(\tilde{\nu})$ (Equations 2 and 3) corresponding to y and z polarized absorbance [19]:

$$A_y(\tilde{\nu}) = (K_y - K_z)^{-1} r_{K_z}(\tilde{\nu}) = -2.273 \cdot r_{0.64}(\tilde{\nu}) \quad (2)$$

$$A_z(\tilde{\nu}) = (K_z - K_y)^{-1} r_{K_y}(\tilde{\nu}) = +2.273 \cdot r_{0.20}(\tilde{\nu}) \quad (3)$$

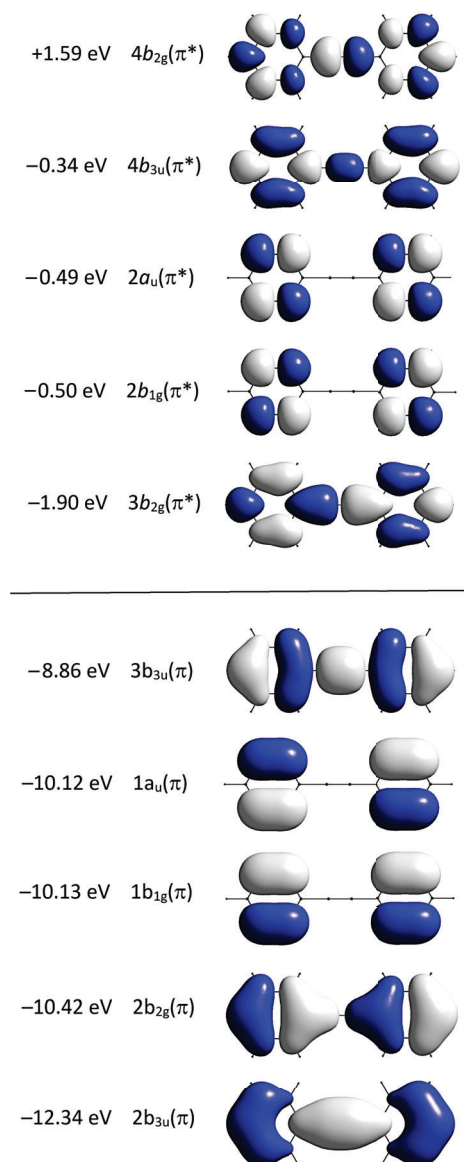


Figure 3. Energies and symmetries of the five highest occupied and five lowest unoccupied π type MOs of diphenylacetylene (DPA) computed with LCOAO with indication of orbital amplitudes.

The resulting partial absorbance curves are shown in Figure 1c. Inspection of the first strong-band system (band A) reveals that the sharp peaks in the vibrational progression in $A_z(\tilde{\nu})$ are associated with S-shaped “wiggles” in $A_y(\tilde{\nu})$. This phenomenon is often observed in reduction procedures with sharp peaks and can be explained by orientation-dependent inhomogeneous line-broadening (different solvent effects for differently oriented solute molecules) [17,18].

3.2. Electronic transitions

3.2.1. Main bands

The wavenumbers, relative absorbance, and polarization directions for the main band systems A, B, C, and D are listed in Table 1, where they are compared with the transitions computed with LCOAO (see also Figure 2 and Sup. S4).

The spectrum starts with a strong band A with an onset at 33,200 cm^{-1} (301 nm). It is z-polarized and must be assigned to the 1^1B_{1u} state predicted by LCOAO at 34,100 cm^{-1} (293 nm) (Table 1). It is well described by the HOMO-LUMO excitation,

$3b_{3u}(\pi) \rightarrow 3b_{2g}(\pi^*)$ (Figure 3). Similar results are obtained with TD-CAM-B3LYP (Table 2).

The next band B with an onset at 44,400 cm^{-1} (225 nm) has a partly resolved vibrational fine structure and a long and diffuse tail towards larger wavenumbers, overlapping the bands C and D. It is y-polarized and can be assigned to the 2^1B_{2u} state computed by LCOAO at 48,700 cm^{-1} (205 nm). This transition is essentially due to the promotions $1a_u(\pi) \rightarrow 3b_{2g}(\pi^*)$ and $3b_{3u}(\pi) \rightarrow 2b_{1g}(\pi^*)$ (SHOMO-LUMO and HOMO-SLUMO). Very similar results are predicted with TD-CAM-B3LYP (Table 2). The wavenumber of this transition is somewhat overestimated by the present calculations. A corresponding situation was observed for (*E*)-1,2-diphenylethene (*trans*-stilbene), which is π iso-electronic with DPA [44].

Band C has a broad z-polarized maximum around 51,000 cm^{-1} (196 nm). It is easily assigned to the 2^1B_{1u} state predicted by LCOAO at 52,200 cm^{-1} (192 nm) (Table 1), primarily involving the orbitals next to the frontier region: $1a_u(\pi) \rightarrow 2b_{1g}(\pi^*)$ and $1b_{1g}(\pi) \rightarrow 2a_u(\pi^*)$ (Figure 3). Again, the results are consistent with those obtained with TD-CAM-B3LYP (Table 2).

The band *D* peaking at 57,100 cm⁻¹ (175 nm) in the vacuum UV region is predominantly *y*-polarized. It can possibly be assigned to the 4¹B_{2u} state predicted by LCOAO at 60,800 cm⁻¹ (164 nm) (Table 1). With the AUG-cc-pVTZ basis set, TD-CAM-B3LYP introduces additional states in this region; the 4¹B_{2u} state predicted by LCOAO therefore corresponds to the 5¹B_{2u} state computed with TD-CAM-B3LYP at 61,000 cm⁻¹ (164 nm) (Table 2). But TD-CAM-B3LYP predicts a strong *z*-polarized transition at 58,300 cm⁻¹ (172 nm), which seems in poor agreement with the observed spectrum (Sup. S2). In any case, the theoretical prediction of electronic states in the vacuum UV is difficult, and the suggested assignment of the absorbance observed in this region must be considered as tentative.

3.2.2. Additional transitions

Much attention has been devoted to the 1¹A_u state of DPA which is of prime importance in the photochemistry of the compound [6-13]. TD-CAM-B3LYP predicts this state at 42,500 cm⁻¹ (235 nm) (Table 2) primarily due to the promotion 8*b*_{2u}(π_{C≡C}) → 3*b*_{2g}(π*), where π_{C≡C} indicates the in-plane π component of the triple-bond. In ground state absorption spectroscopy, the state is optically forbidden in the D_{2h} point group, but it gains intensity in distorted conformations. Comparison with the optical properties of the “molecular rotor” diphenyldiacetylene (DPDA, Scheme 1) seems relevant [15].

Apart from the 1¹B_{1u} state responsible for band *A*, the lowest optically allowed state is predicted to be 1¹B_{2u}. LCOAO and TD-CAM-B3LYP predict this state at 36,700 cm⁻¹ (272 nm) and 40,900 cm⁻¹ (244 nm), respectively (Tables 1 and 2). The leading configurations are 1*a*_u(π) → 3*b*_{2g}(π*) and 3*b*_{3u}(π) → 2*b*_{1g}(π*), similar to the 2¹B_{2u} state giving rise to band *B*. The 1¹B_{2u} and 2¹B_{2u} states are essentially *minus* and *plus* combinations of the two configurations, a consequence of the approximate pairing symmetry [25,26,45] of the DPA π system. Because of the *minus* character, the transition to the 1¹B_{2u} state is predicted to be weak (“parity forbidden”) and it is likely to be buried under the strong absorbance due to the 1¹B_{1u} state (band *A*). The transition may possibly be observed directly in the MCD spectrum, since positive and negative B-terms are predicted for 1¹B_{1u} and 1¹B_{2u} (Table 1, Figure 2, Sup. S4).

It should be mentioned that a variety of CAS-based procedures predict 1¹B_{2u} as the lowest excited singlet state [7,12]. The present calculations clearly predict 1¹B_{1u} as the lowest excited singlet state of DPA, in agreement with the results of semiempirical [5,6], TD-DFT [8,12], and ADC(2) [10] calculations. See the detailed discussion by Robertson and Worth [12].

LCOAO predicts the 3¹B_{2u} state in the vacuum UV at 56,100 cm⁻¹ (178 nm) (Table 1). The corresponding state computed with TD-CAM-B3LYP is 4¹B_{2u} at 59,500 cm⁻¹ (168 nm) (Table 2). This state is not clearly observed in the present spectrum, but it may contribute to the *y*-polarized absorbance in the region between the bands *B* and *D*, possibly gaining intensity by vibronic coupling with these strong bands. It may possibly be observed in the MCD spectrum, since a large negative B-term is predicted for this state (Table 1, Figure 2). However, as indicated above, the results in the high-wavenumber region should be treated with caution.

4. Conclusions

The absorbance spectrum of diphenylacetylene (DPA) is characterized by four characteristic bands *A*, *B*, *C*, and *D* in the region 58,000–28,000 cm⁻¹ (172–360 nm), similar to the spectrum of *trans*-stilbene [44]. According to the present results, bands *A* and *C* are *z*-polarized, while bands *B* and *D* are *y*-polarized. The LCOAO model provides an adequate theoretical description of the four main bands. The TD-CAM-B3LYP results are consistent with those obtained with LCOAO,

except in the region of band *D* in the vacuum UV, where the two methods differ in the prediction of individual electronic transitions. The optically allowed states 1¹B_{2u} and 3¹B_{2u} are predicted with too low intensity to be observed in the present experimental spectra, but the MCD B-terms predicted by LCOAO suggest that they may be observed by MCD spectroscopy.

Acknowledgements

This investigation was supported by grants of beam time on the CD1 beamline at the Centre for Storage Ring Facilities (ISA), Aarhus University. The stay of Nguyen Duc Duy at Roskilde University was enabled by a Ph.D. scholarship granted by the Vietnamese Ministry of Education and Training. The Danish International Development Agency (DANIDA) provided additional support via the Enhancement of Research Capacity (ENRECA) program. The authors are grateful to Signe Høgsberg Andersen for preliminary investigations of the title compound and to Eva M. Karlsen for technical assistance in the spectroscopy laboratory.

Supporting information S

Electronic supplementary material available: Spectroscopic peak data. Nuclear equilibrium coordinates calculated with CAM-B3LYP/AUG-cc-pVTZ and CAM-B3LYP/cc-pVTZ. Complete list and graphical representations of electronic transitions predicted with TD-CAM-B3LYP/AUG-cc-pVTZ, TD-CAM-B3LYP/cc-pVTZ and LCOAO. LCOAO bibliography 1980-2023.

Disclosure statement DS

Conflict of interest: The authors declare that they have no conflict of interest. Ethical approval: All ethical guidelines have been adhered to. Data availability: Spectroscopic data are available from the UV/Vis+ Photochemistry Data Base (<https://science-softcon.de/spectra/>).

CRediT authorship contribution statement CR

Conceptualization: Duy Duc Nguyen, Jens Spanget-Larsen; Methodology: Duy Duc Nguyen, Jens Spanget-Larsen; Formal Analysis: Jens Spanget-Larsen; Investigation: Duy Duc Nguyen, Nykola C. Jones, Søren Vronning Hoffmann, Jens Spanget-Larsen; Resources: Nykola C. Jones, Søren Vronning Hoffmann, Jens Spanget-Larsen; Data Curation: Jens Spanget-Larsen; Writing - Original Draft: Jens Spanget-Larsen; Writing - Review and Editing: Nykola C. Jones, Søren Vronning Hoffmann, Jens Spanget-Larsen; Visualization: Jens Spanget-Larsen.

ORCID ID and Email

Duy Duc Nguyen
 duy.nguyen@intertek.com
 <https://orcid.org/0009-0002-4241-8256>
 Nykola C. Jones
 nykj@phys.au.dk
 <https://orcid.org/0000-0002-4081-6405>
 Søren Vronning Hoffmann
 vronning@phys.au.dk
 <https://orcid.org/0000-0002-8018-5433>
 Jens Spanget-Larsen
 spanget@ruc.dk
 <https://orcid.org/0000-0002-4212-7603>

References

- Bunz, U. H. F. Poly(aryleneethynylene)s: Syntheses, properties, structures, and applications. *Chem. Rev.* **2000**, *100*, 1605–1644.
- Li, Y.; Zhao, J.; Yin, G. Theoretical investigations of oligo(phenylene ethylene) molecular wire: Effects from substituents and external electric field. *Comput. Mater. Sci.* **2007**, *39*, 775–781.
- Whitten, D. G.; Tang, Y.; Zhou, Z.; Yang, J.; Wang, Y.; Hill, E. H.; Pappas, H. C.; Donabedian, P. L.; Chi, E. Y. A retrospective: 10 years of oligo(phenylene-ethynylene) electrolytes: Demystifying nanomaterials. *Langmuir* **2019**, *35*, 307–325.
- Chen, H.; Sangtarash, S.; Li, G.; Gantenbein, M.; Cao, W.; Alqorashi, A.; Liu, J.; Zhang, C.; Zhang, Y.; Chen, L.; Chen, Y.; Olsen, G.; Sadeghi, H.; Bryce, M. R.; Lambert, C. J.; Hong, W. Exploring the thermoelectric

- properties of oligo(phenylene-ethynylene) derivatives. *Nanoscale* **2020**, *12*, 15150–15156.
- [5]. Gutmann, M.; Gudipati, M.; Schoenart, P. F.; Hohlneicher, G. Electronic spectra of matrix-isolated tolan: site selective one- and two-photon spectra. *J. Phys. Chem.* **1992**, *96*, 2433–2442.
 - [6]. Ferrante, C.; Kensy, U.; Dick, B. Does diphenylacetylene (tolan) fluoresce from its second excited singlet state? Semiempirical MO calculations and fluorescence quantum yield measurements. *J. Phys. Chem.* **1993**, *97*, 13457–13463.
 - [7]. Amatatsu, Y.; Hosokawa, M. Theoretical study on the photochemical behavior of diphenylacetylene in the low-lying excited states. *J. Phys. Chem. A* **2004**, *108*, 10238–10244.
 - [8]. Zgierski, M. Z.; Lim, E. C. Nature of the 'dark' state in diphenylacetylene and related molecules: state switch from the linear $\pi\pi^*$ state to the bent $\pi\sigma^*$ state. *Chem. Phys. Lett.* **2004**, *387*, 352–355.
 - [9]. Satiel, J.; Kumar, V. K. R. Photophysics of diphenylacetylene: Light from the "dark state." *J. Phys. Chem. A* **2012**, *116*, 10548–10558.
 - [10]. Krämer, M.; Bunz, U. H. F.; Dreu, A. Comprehensive look at the photochemistry of tolane. *J. Phys. Chem. A* **2017**, *121*, 946–953.
 - [11]. Ho, E. K.-L.; Etienne, T.; Lasorne, B. Vibronic properties of *para*-polyphenylene ethynylenes: TD-DFT insights. *J. Chem. Phys.* **2017**, *146*, 164303.
 - [12]. Robertson, C.; Worth, G. A. Modelling the non-radiative singlet excited state isomerization of diphenyl-acetylene: A vibronic coupling model. *Chem. Phys.* **2018**, *510*, 17–29.
 - [13]. Flock, M.; Bosse, L.; Kaiser, D.; Engels, B.; Fischer, I. A time-resolved photoelectron imaging study on isolated tolane: observation of the biradicalic 1A_u state. *Phys. Chem. Chem. Phys.* **2019**, *21*, 13157–13164.
 - [14]. Fan, L.-X.; Chen, L.; Zhang, H.-Y.; Xu, W.-H.; Wang, X.-L.; Xu, S.; Wang, Y.-Z. Dual photo-responsive diphenylacetylene enables PET in-situ upcycling with reverse enhanced UV-resistance and strength. *Angew. Chem. Int. Ed Engl.* **2023**, *62*, e202314448.
 - [15]. Thulstrup, P. W.; Hoffmann, S. V.; Hansen, B. K. V.; Spanget-Larsen, J. Unique interplay between electronic states and dihedral angle for the molecular rotor diphenyldiacetylene. *Phys. Chem. Chem. Phys.* **2011**, *13*, 16168–16174.
 - [16]. Nguyen, D. D.; Jones, N. C.; Hoffmann, S. V.; Andersen, S. H.; Thulstrup, P. W.; Spanget-Larsen, J. Electronic states of 1,4-bis(phenylethynyl)benzene: A synchrotron radiation linear dichroism investigation. *Chem. Phys.* **2012**, *392*, 130–135.
 - [17]. Michl, J.; Thulstrup, E. W. *Spectroscopy with polarized light: Solute alignment by photoselection, liquid crystal, polymers, and membranes corrected software edition*; John Wiley & Sons: Nashville, TN, 1995.
 - [18]. Thulstrup, E. W.; Michl, J. *Elementary polarization spectroscopy*; John Wiley & Sons: Nashville, TN, 1997.
 - [19]. Madsen, F.; Terpager, I.; Olskær, K.; Spanget-Larsen, J. Ultraviolet-visible and infrared linear dichroism spectroscopy of 1,8-dihydroxy-9,10-anthraquinone aligned in stretched polyethylene. *Chem. Phys.* **1992**, *165*, 351–360.
 - [20]. Rodger, A.; Norden, B. *Circular Dichroism and Linear Dichroism*; Oxford University Press: London, England, 1996.
 - [21]. Nordén, B.; Rodger, A.; Dafforn, T. *Linear dichroism and circular dichroism: A textbook on polarized-light spectroscopy*; Royal Society of Chemistry: Cambridge, England, 2023.
 - [22]. Thulstrup, E. W.; Waluk, J.; Spanget-Larsen, J. *Encyclopedia of spectroscopy and spectrometry*; third edition, J.C. Lindon, G.E. Tranter, D.W. Koppenaal, Eds. Academic Press, Oxford, UK, 2017. pp 595-600.
 - [23]. Miles, A. J.; Hoffmann, S. V.; Tao, Y.; Janes, R. W.; Wallace, B. A. Synchrotron Radiation Circular Dichroism (SRCD) spectroscopy: New beamlines and new applications in biology. *Spectrosc. Int. J.* **2007**, *21*, 245–255.
 - [24]. Miles, A. J.; Janes, R. W.; Brown, A.; Clarke, D. T.; Sutherland, J. C.; Tao, Y.; Wallace, B. A.; Hoffmann, S. V. Light flux density threshold at which protein denaturation is induced by synchrotron radiation circular dichroism beamlines. *J. Synchrotron Radiat.* **2008**, *15*, 420–422.
 - [25]. Spanget-Larsen, J. The alternant hydrocarbon pairing theorem and all-valence electrons theory. An approximate LCOAO theory for the electronic absorption and MCD spectra of conjugated organic compounds. 1. *Croat. Chem. Acta.* **1986**, *59*, 711-717. <https://hrcak.srce.hr/file/261320>.
 - [26]. Spanget-Larsen, J. The alternant hydrocarbon pairing theorem and all-valence electrons theory. An approximate LCOAO theory for the electronic absorption and MCD spectra of conjugated organic compounds, part 2. *Theor. Chem. Acc.* **1997**, *98*, 137–153.
 - [27]. Casida, M. E. Time-dependent density-functional theory for molecules and molecular solids. *Theochem* **2009**, *914*, 3–18.
 - [28]. Adamo, C.; Jacquemin, D. The calculations of excited-state properties with Time-Dependent Density Functional Theory. *Chem. Soc. Rev.* **2013**, *42*, 845–856.
 - [29]. Foresman, J. B.; Frisch, A. E. *Exploring chemistry with electronic structure methods*; third edition, Gaussian Inc, Wallingford CT, 2015.
 - [30]. Yanai, T.; Tew, D. P.; Handy, N. C. A new hybrid exchange–correlation functional using the Coulomb-attenuating method (CAM-B3LYP). *Chem. Phys. Lett.* **2004**, *393*, 51–57.
 - [31]. Michl, J. Magnetic circular dichroism of aromatic molecules. *Tetrahedron* **1984**, *40*, 3845–3934.
 - [32]. Thulstrup, P. W.; Jones, N. C.; Hoffmann, S. V.; Spanget-Larsen, J. Electronic states of the fluorophore 9,10-bis(phenylethynyl)anthracene (BPEA). A synchrotron radiation linear dichroism investigation. *Chem. Phys. Lett.* **2013**, *559*, 35–40.
 - [33]. Thulstrup, P. W.; Jones, N. C.; Hoffmann, S. V.; Spanget-Larsen, J. UV polarisation spectroscopy of 1,4-diethynylbenzene. *Mol. Phys.* **2021**, *119*, e1853841.
 - [34]. PhotochemCAD: 1,2-diphenylacetylene. <https://omlc.org/spectra/PhotochemCAD/html/114.html> (accessed August 28, 2023).
 - [35]. Spanget-Larsen, J. LCOAO Computer Program: Fortran source code with sample input and output, *ResearchGate* 2005, <http://dx.doi.org/10.13140/2.1.3455.6482>
 - [36]. Frisch, M. J.; Trucks, G. W.; Schlegel, H. B.; Scuseria, G. E.; Robb, M. A.; Cheeseman, J. R.; Scalmani, G.; Barone, V.; Petersson, G. A.; Nakatsuji, H.; Li, X.; Caricato, M.; Marenich, A. V.; Bloino, J.; Janesko, B. G.; Gomperts, R.; Mennucci, B.; Hratchian, H. P.; Ortiz, J. V.; Izmaylov, A. F.; Sonnenberg, J. L.; Williams-Young, D.; Ding, F.; Lipparini, F.; Egidi, F.; Goings, J.; Peng, B.; Petrone, A.; Henderson, T.; Ranasinghe, D.; Zakrzewski, V. G.; Gao, J.; Rega, N.; Zheng, G.; Liang, W.; Hada, M.; Ehara, M.; Toyota, K.; Fukuda, R.; Hasegawa, J.; Ishida, M.; Nakajima, T.; Honda, Y.; Kitao, O.; Nakai, H.; Vreven, T.; Throssell, K.; Montgomery, J. A., Jr.; Peralta, J. E.; Ogliaro, F.; Bearpark, M. J.; Heyd, J. J.; Brothers, E. N.; Kudin, K. N.; Staroverov, V. N.; Keith, T. A.; Kobayashi, R.; Normand, J.; Raghavachari, K.; Rendell, A. P.; Burant, J. C.; Iyengar, S. S.; Tomasi, J.; Cossi, M.; Millam, J. M.; Klene, M.; Adamo, C.; Cammi, R.; Ochterski, J. W.; Martin, R. L.; Morokuma, K.; Farkas, O.; Foresman, J. B.; Fox, D. J. Gaussian 16, Revision A.03, Gaussian, Inc., Wallingford CT, 2016.
 - [37]. Dunning, T. H., Jr Gaussian basis sets for use in correlated molecular calculations. I. The atoms boron through neon and hydrogen. *J. Chem. Phys.* **1989**, *90*, 1007–1023.
 - [38]. Kendall, R. A.; Dunning, T. H., Jr; Harrison, R. J. Electron affinities of the first-row atoms revisited. Systematic basis sets and wave functions. *J. Chem. Phys.* **1992**, *96*, 6796–6806.
 - [39]. Miertuš, S.; Scrocco, E.; Tomasi, J. Electrostatic interaction of a solute with a continuum. A direct utilization of AB initio molecular potentials for the prevision of solvent effects. *Chem. Phys.* **1981**, *55*, 117–129.
 - [40]. Tomasi, J.; Persico, M. Molecular interactions in solution: An overview of methods based on continuous distributions of the solvent. *Chem. Rev.* **1994**, *94*, 2027–2094.
 - [41]. Cramer, C. J.; Truhlar, D. G. Implicit solvation models: Equilibria, structure, spectra, and dynamics. *Chem. Rev.* **1999**, *99*, 2161–2200.
 - [42]. Scalmani, G.; Frisch, M. J. Continuous surface charge polarizable continuum models of solvation. I. General formalism. *J. Chem. Phys.* **2010**, *132*, 114110.
 - [43]. Grimme, S.; Ehrlich, S.; Goerigk, L. Effect of the damping function in dispersion corrected density functional theory. *J. Comput. Chem.* **2011**, *32*, 1456–1465.
 - [44]. Nguyen, D. D.; Jones, N. C.; Hoffmann, S. V.; Spanget-Larsen, J. Excited states of *trans*-stilbene and 1,4-diphenylbutadiene. Near and vacuum UV polarization spectroscopy. *J. Mol. Struct.* **2023**, *1293*, 136206.
 - [45]. Pariser, R. Theory of the electronic spectra and structure of the polyacenes and of alternant hydrocarbons. *J. Chem. Phys.* **1956**, *24*, 250–268.



Copyright © 2024 by Authors. This work is published and licensed by Atlanta Publishing House LLC, Atlanta, GA, USA. The full terms of this license are available at <https://www.eurjchem.com/index.php/eurjchem/terms> and incorporate the Creative Commons Attribution-Non Commercial (CC BY NC) (International, v4.0) License (<http://creativecommons.org/licenses/by-nc/4.0>). By accessing the work, you hereby accept the Terms. This is an open access article distributed under the terms and conditions of the CC BY NC License, which permits unrestricted non-commercial use, distribution, and reproduction in any medium, provided the original work is properly cited without any further permission from Atlanta Publishing House LLC (European Journal of Chemistry). No use, distribution, or reproduction is permitted which does not comply with these terms. Permissions for commercial use of this work beyond the scope of the License (<https://www.eurjchem.com/index.php/eurjchem/terms>) are administered by Atlanta Publishing House LLC (European Journal of Chemistry).